Special Collection

Electrochemical Reduction of 4-Nitrobenzyl Phenyl Thioether for Activation and Capture of CO_2

Silvia Mena, Cyril Louault, Verónica Mesa, Iluminada Gallardo,* and Gonzalo Guirado*[a]

In this work, a new simple molecule, 4-nitrobenzyl phenyl thioether (**1**), is prepared and used for controlling and tuning CO_2 reactivity in function of the electrode potential. The first part of the study is devoted to determining the electrochemical reduction mechanism of **1** in *N,N*-dimethylformamide under nitrogen. The compound shows a first reversible one-electron transfer process, whereas the reaction cleavage of the C–S bond takes place after a second electron transfer process through a stepwise mechanism (thermodynamic and kinetic parameters are conveniently determined). In the second part of the study, the inert atmosphere was replaced by a CO_2 atmosphere. At low potential values, compound **1** acts as a redox mediator that allows the reduction of CO_2 at ca. −1.2 V vs. SCE. The electrochemical generation of 1^{2-} at more negative potential values leads to a C–S bond cleavage reaction that yields the corresponding nitrobenzyl and thiosulfate anions, which react with CO_2. The nitro aromatic anion derivative makes it possible to obtain electrocarboxylated derivatives, whereas the thiophenolate anion captures CO_2 reversibly. Hence, this research opens a new way of tuning and controlling the reaction processes associated with CO_2 from homogenous catalysis at low negative potentials, to electrocarboxylation processes passing to CO_2 reversible electrochemically triggered adsorption processes.

1. Introduction

There has been growing interest in activation and cleavage of the carbon–sulfur bond due to its role in the field of fuel, coal industry, bioorganic and synthesis for decades.[1–3] There are many ways to activate and cleave C–heteroatom bonds, such as with transition metals.[4,5] However, this chemistry requires high loading of toxic and air-sensitive transition metals and extremely high temperatures and is only feasible with more reactive methyl and ethyl esters.[6] Electrochemistry has been widely used in the activation and cleavage of C–heteroatom bonds. The electron-transfer reaction may lead to chemically stable species and to bond cleavage or bond formation. General reactivity models have been constructed for this kind of reaction. There are extensive reports on the mechanisms of carbon–halogen bond cleavage.[7–11] The general mechanism consists in the electrochemical activation of organic molecules (A–B) by producing a radical anion after the electron transfer, which cleaves to produce a radical and an anion in two steps (stepwise process) or in a one-step (concerted process) pathway (Scheme 1).

The strength of the carbon–halogen bond, the leaving group ability of the resultant anion and the reaction medium play important roles in determining the preferred process.[12] Similarly, different bond cleavages have been researched, notably the C–O and C–S bond cleavages in ether and thioether.[1,13–17] These bond cleavages have a particular interest in different biological phenomenon, such as in the DNA stand break of the $C_{3'}$–$O_{3'}$ bond,[18] or for photocleavage of the benzyl–sulfide bond in a ribonucleoside, which is interesting for its successful photoaffinity labelling of a membrane transport protein.[19] Focusing on the C–S bond cleavage reaction, Singh et al.[20] recently found that it is possible to generate benzylthiolate anion moieties ($PhCH_2S^-$) through an electrochemical reduction process of benzyldisulfide ($PhCH_2$–S–S–CH_2Ph) of high-negative potentials, and these benzylthiolate anions are able to reversibly capture CO_2 (Scheme 2).

Electrochemistry methods can also be used to perform carboxylation reactions, and have been widely studied as a "greener" alternative to chemical methods.[21–23] Hence, the use of CO_2 as a feedstock is a promising strategy for obtaining

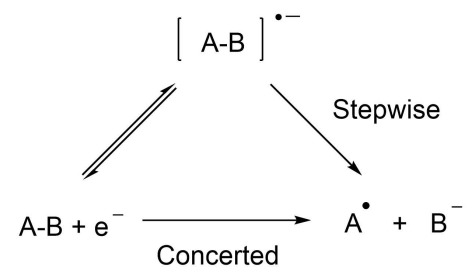

Scheme 1. Electrochemically triggered dissociative electron transfer pathways.

[a] *Dr. S. Mena, Dr. C. Louault, V. Mesa, Prof. I. Gallardo, Dr. G. Guirado*
Departament de Química
Universitat Autònoma de Barcelona
Campus UAB, 08193-Bellaterra, Barcelona, Spain
E-mail: iluminada.gallardo@uab.cat
gonzalo.guirado@uab.cat

Supporting information for this article is available on the WWW under https://doi.org/10.1002/celc.202100329

An invited contribution to a joint Special Collection in memory of Prof. Jean-Michel Savéant

© 2021 The Authors. ChemElectroChem published by Wiley-VCH GmbH. This is an open access article under the terms of the Creative Commons Attribution Non-Commercial License, which permits use, distribution and reproduction in any medium, provided the original work is properly cited and is not used for commercial purposes.

carboxylic acids *via* electrochemical fixation of CO_2. Moreover, CO_2 can be easily incorporated into the organic skeleton under mild conditions by using suitable electrodes, electrolytes and catalysts in the electrolysis. In terms of green and sustainable chemistry, this approach is essentially environmentally benign and carbon dioxide is an eco-friendly C1 source.[24–27] Usually, electrocarboxylation reactions of organic compounds using CO_2 are carried out through two different reaction pathways. The first one involves the electrochemical generation of organic anionic intermediates on the passage of two electrons, which undergo a nucleophilic attack on carbon dioxide to yield the corresponding carboxylic acids [Scheme 3, Eqs. (1)–(4)]. This pathway takes place when the reduction potentials of the organic substrates are less negative than that of carbon dioxide ($E_{reduction,\ CO2} = -2.2$ V vs SCE). The second approach is based on the reactivity of the CO_2 radical anion and can take place when the reduction potentials of the organic substrates are more negative than the carbon dioxide reduction potential. This mechanism describes the electrogeneration of the radical anion of carbon dioxide,[28] which can be generated directly on the surface of the cathodic electrode [Scheme 3, Eq. (5)], or through a homogeneous catalysis in a bulk solution with an organic mediator [Scheme 3, Eq. (5′)]. This radical anion reacts with organic substrates leading to the corresponding carboxylic acids [Scheme 3, Eqs. (6)–(8)].

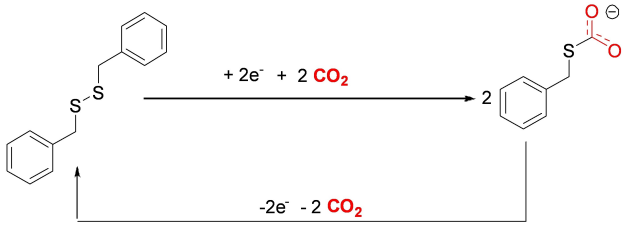

Scheme 2. Electrochemical cycle that enables capture and release of carbon dioxide with the use of benzylthiolate as capture agent.

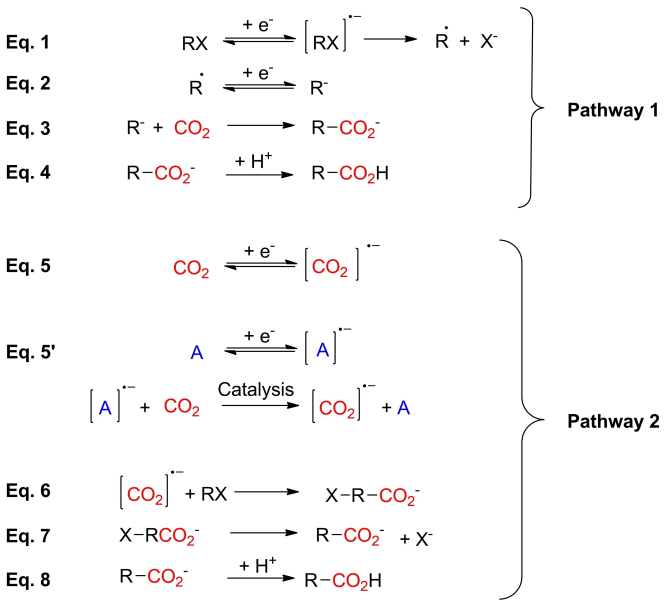

Scheme 3. Electrocarboxylation reactions of organic compounds using CO_2.

It is important to remember that the use of electrochemical methods also makes electro-reducing carbon dioxide possible, but with a homogeneous catalyst based on organic molecules (A). Radical anion of aromatic nitriles,[26,29] esters,[29] and recently electrochemically-generated nitrocompounds[30] have the remarkable property of reducing CO_2 to its radical anion specie, $CO_2^{\bullet-}$. This radical anion would eventually evolve leading to different CO_2 reduction products depending on the experimental conditions (Scheme 4).

Hence, the aim of this work is to design a new molecule for controlling and tuning the CO_2 reactivity in function of the electrode potential. Therefore, it seems to be possible to use electrochemical control for activating, capturing and valorizing CO_2 with the 4-nitrobenzyl phenyl thioether (**1**) (Figure 1), an

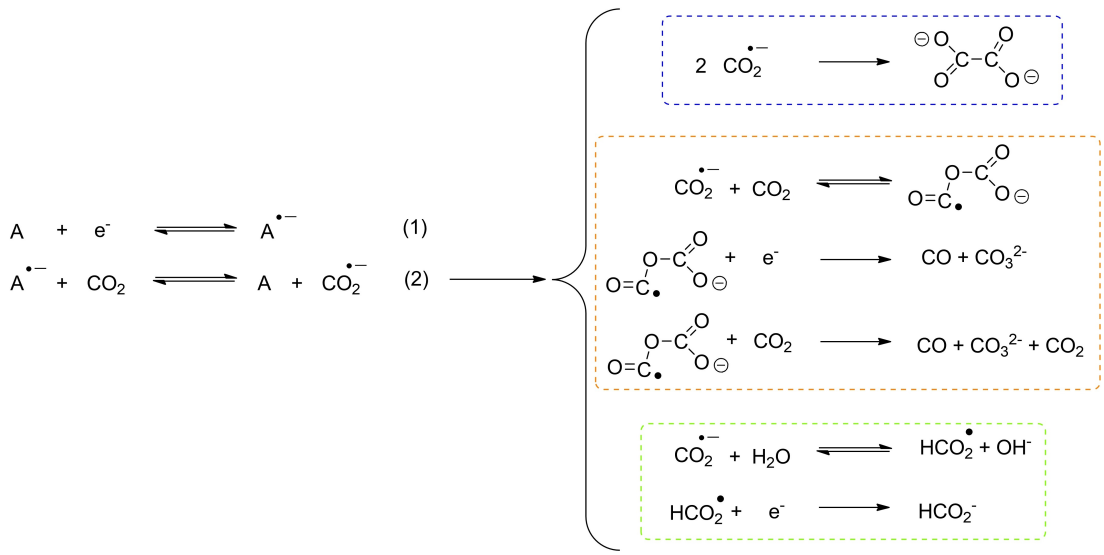

Scheme 4. Electroreduction of CO_2 with the organic molecule as the homogeneous catalyst.

© 2021 The Authors. ChemElectroChem published by Wiley-VCH GmbH

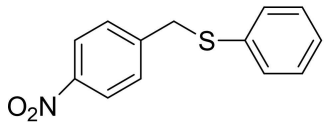

Figure 1. 4-Nitrobenzyl phenyl thioeter, **1**.

aryl–thioether compound with a nitro group substituent. Introducing a nitro substituent into the aromatic ring makes it possible to obtain a stable radical anion, which can potentially act as a redox mediator for CO_2 activation. Moreover, in a second electron transfer process the dianion, $\mathbf{1}^{2-}$, can occur through the C–S bond cleavage reaction, leading to the corresponding nitrobenzyl and thiosulfate anions. The electrochemical generation of the nitrobenzyl anion may react with CO_2 to yield an electrocarboxylated product, whereas the thiophenolate anion could also reversibly capture CO_2.

Experimental Section

Chemicals

Reagents

4-nitrobenzyl bromide and sodium thiophenolate were obtained from Sigma-Aldrich and were the highest purity available.

Reactant Gases

Carbon dioxide (CO_2) and nitrogen and argon were purchased from Carburos Metalicos S.A. with a purity of 99.9999%.

Solvent and supporting electrolyte

Dichloromethane, methanol, ethanol, toluene and pentane were obtained from SDS. All chemicals were used as received.

N,N′-dimethylformamide, DMF anhydrous, 99.8% (SigmaAldrich) and the supporting electrolyte, tetrabutylammonium tetrafluoroborate, $TBABF_4$, (Aldrich) were used as received without further purification.

4-nitrobenzyl phenyl thioether, 1

Compound **1** was prepared by the reaction between 4-nitrobenzylbromide (0.176 g, 0.82 mmol) and sodium thiophenolate (1.078 g, 8.16 mmol) in dichloromethane under an inert atmosphere. The mixture was stirred for 48 h at room temperature. The solution obtained was poured into water and extracted three times with dichloromethane. Organic layers were reunited and dried over sodium sulfate anhydrous. The residue after solvent evaporation was purified using a silica gel chromatography column with a n-pentane/dichloromethane (3:2) mixture and produced the desired product as a light yellow solid (60% yield).

^{1}H-NMR ($CDCl_3$): δ (ppm) 8.12 (d, J = 8.6 Hz, 2H), 7.38 (d, J = 8.6 Hz, 2H), 7.27 (m, 5H), 4.14 (s, 2H).

GC-MS (70 eV): m/z (%) 245 (100) [M^+], 199 (19) [$M^+ - NO_2$], 136 (49) [$C_7H_6NO_2\cdot$], 120 (13), 109 (14) [$C_6H_5S\cdot$], 106 (23), 90 (21) [$C_7H_6^{2}\cdot$], 89 (20), 78 (24).

Instruments and procedures

^{1}H NMR spectra were recorded on a Brucker DPX250 spectrometer operating at 250,13 MHz (Billerica, MA, USA). Proton chemical shifts were reported in ppm (δ) (CD_3CN, δ = 1.98). The J values were reported in Hz.

Gas phase chromatography were performed with a Clarus 500 from Perkin Elmer (vector gas: Helium, column: Elite 5, l = 30 m, d = 0.25 mm). A Hewlett Packard 6890 apparatus was used for gas phase chromatography coupled with mass spectrometry. The flame ionization detector (FID) was a Hewlett Packard 5973.

Products obtained after electrolysis were analyzed by the Servei d'Analisis Quimica (SAQ) of the Autonomous University of Barcelona (UAB) by GC-MS (gas phase chromatography GC 6890, Agilent Technologies, with mass spectroscopy Hewlett-Packard 5973).

Electrochemical procedures

Electrochemical measurements were performed in a one-compartment cell using the three-electrode configuration. The working electrode was a 1 mm diameter glassy carbon electrode disk carefully polished with 1 μm diamond paste (DP-Paste, P) and rinsed with ethanol. The counter electrode was a 2 mm platinum electrode disk and the reference electrode a Saturated Calomel Electrode (SCE) separated from the solution by a sintered-glass disk (salt-bridge). Therefore, all potentials were reported compared to this reference. All experiments were carried out at 15 °C, and the double wall jacketed cell was thermostated by circulation of methanol.

The solution to be studied was prepared by dissolving the substrate in a solution containing the solvent (DMF) and 0.10 $mol\cdot L^{-1}$ of support electrolyte ($TBABF_4$), except for fast cyclic (scan rate (v) greater than 100 $V\cdot s^{-1}$) for which the concentration of the support electrolyte is 0.60 $mol\cdot L^{-1}$. The substrate concentration was a few millimoles per liter and the volume of the solution was 10 mL. Between taking records, the solution was stirred by a current of argon in order to homogenize the solution and remove the oxygen.

Cyclic voltammetry was recorded using a potentiostat equipped with positive feedback compensation and current measurer. The triangular signal is delivered by a TACUSSEL generator type GSTP 4. An electronic system compensates the resistance (R_u) between the working electrode and the reference electrode. The voltammograms are first recorded on a TEKTRONIX 2212 digital oscilloscope and then transcribed to paper using a HEWLETT PACKARD 7475 A plotter.

Controlled potential electrolysis was carried out using a potentiostat EG&G PRINCETON APPLIED RESEARCH model 273 A. The same electrochemical cell, as it was previously described for cyclic voltammetry, has been used for controlled potential electrolysis experiments. However, in this case the working electrode was a graphite rod (area: 8.1 cm^2); the counter electrode a platinum wire and the reference electrode a SCE electrode. Counter and reference electrodes were separated from the solution by a salt bridge. This salt-bridge ends in a frit, which is made of a ceramic material, avoiding appreciable contamination.

Controlled potential electrolysis and electrocarboxylation reactions were performed under either nitrogen or argon and CO_2 atmosphere, respectively. For electrocarboxylation reactions a Mass Flow

© 2021 The Authors. ChemElectroChem published by Wiley-VCH GmbH

Meter was used to control the CO_2 concentrations and flows. All experiments were also monitored using Cyclic Voltammetry. After electrolysis, water was added to the solution. The aqueous phase was extracted three times with toluene. The combined organic phases were dried with anhydrous sulfate sodium. The solvent was removed under a high vacuum. The residue was dissolved in dichloromethane and characterized by gas chromatography-mass spectrometry (GC-MS) and Proton Nuclear Magnetic Resonance (^{1}H-RMN).

Thiophenol: *^{1}H-NMR ($CDCl_3$): δ (ppm)* 7.35–7.31 (m, 4H), 7.20 (t, J = 6.9 Hz, 1H), 3.50 (s, 1H). *GC-MS (70 eV): m/z (%)* 110 (100) [M^+], 109 (24.1) [M^+ –H], 77 (12.3) [M^+ –SH], 66 (31), 65 (10.7).

4-nitrotoluene: *^{1}H-NMR ($CDCl_3$): δ (ppm)* 8.10 (d, J = 8.43 Hz, 2H), 7.31 (d, J = 8.43 Hz, 2H), 2.46 (s, 3H). *GC-MS (70 eV): m/z (%)* 137 (75.7) [M^+], 91 (100) [M^+ –NO_2], 77 (11.8) [$C_6H_5^+$], 65 (57.8), 63 (13.7), 39 (21.2).

*Diphenyl disulfide (**2**):* *^{1}H-NMR ($CDCl_3$): δ (ppm)* 7.52 (d, J = 7.52 Hz, 4H), 7.30 (t, J = 7.52 Hz, 4H), 7.24 (t, J = 7.21, 2H). *GC-MS (70 eV): m/z (%)* 218 (100) [M^+], 184.9 (12.1), 140 (5.8) [M^+ –C_6H_5·], 109 (92.2) [M^+ –C_6H_5S·], 65 (27.7), 51 (8.7).

4-nitrobenzaldehyde (p-NO_2–Ph–CHO): *^{1}H-NMR ($CDCl_3$): δ (ppm)* 10.16 (s, 1H), 8.39 (d, J = 8.4 Hz, 2H), 8.07 (d, J = 8.4 Hz, 2H). *GC-MS (70 eV): m/z (%)* 151 (100) [M^+], 150 (86.9) [M^+ –H·], 105 (27.2), 104 (19.4), 77 (68.1) [$C_6H_5^+$], 65 (11.1), 51 (63.4), 50 (28.3).

4,4′-dinitrobibenzyl, D1: *^{1}H-NMR ($CDCl_3$): δ (ppm)* 8.08 (d, J = 8.5 Hz, 4H), 7.22 (d, J = 12.7 Hz, 4H), 3.6 (s, 4H). *GC-MS (70 eV): m/z (%)* 272 (46.9) [M^+], 226 (10.8) [M^+ –NO_2], 178 (4.8), 136 (100) [$C_7H_6NO_2^{2\cdot}$], 106 (24.5), 90 (10.9) [$C_7H_6^{2\cdot}$].

4,4′-dinitrostilbene, D2: *^{1}H-NMR ($CDCl_3$): δ (ppm)* 8.29 (d, J = 8.9 Hz, 4H), 7.72 (d, J = 8.9 Hz, 4H), 7.33 (s, 2H). *GC-MS (70 eV): m/z (%)* 270 (100) [M^+], 178 (25.9) [M^+ –$2NO_2$], 165 (21.1), 76 (9.2) [$C_6H_4^{2\cdot}$].

*4-aminobenzeneacetic acid (**3**):* *^{1}H-NMR ($CDCl_3$): δ (ppm)* 6.89 (d, J = 7.6 Hz, 2H), 6.50 (d, J = 7.6 Hz, 2H), 3.33 (s, 2H). *GC-MS (70 eV):* m/z (%) 151 (32) [M^+], 106 (100) [M^+ –COOH·], 77 (8.3) [$C_6H_5^+$], 18 (6.6).

*4-[(phenylthio)methyl]benzenamine (**4**):* *^{1}H-NMR ($CDCl_3$): δ (ppm)* 7.34 (m, 4H), 7.20 (m, 3H), 6.69 (d, J = 7.8 Hz, 2H), 4.28 (s, 2H), 4.13 (s, 2H). *GC-MS (70 eV): m/z (%)* 215 (40) [M^+], 106 (100) [M^+ –C_6H_5S·], 77 (84), 65 (30), 51 (19).

Determination of the CO_2 concentration in the solvent

A thermal flow meter of molecular construction with "laboratory style" pc-board housing (EL-FLOW® Mass Flow Meter/Controller, Bronkhorst Hi-Tec) was employed for monitoring the CO_2 concentration in the solution. Control valves were included to measure and control the flow from the lowest range of 0.2–1 mL/min.

2. Results and Discussion

2.1. Electrochemical Study of 4-Nitrobenzyl Phenyl Thioether Under Inert Atmosphere

Compound **1** was electrochemically studied by cyclic voltammetry (CV) under an inert atmosphere. The typical CV of a 5 mM solution of compound **1** in DMF/0.1 M $TBABF_4$ is depicted in Figure 2 at different scan ranges.

A cathodic scan, up to −2.7 V, shows three different electron transfers. A first monoelectronic fast reversible electron transfer, with $E_{pc,1} = -1.12$ V (vs SCE), followed by a second irreversible electron transfer, $E_{pc,2} = -2.0$ V (vs SCE), and a third multi-electron irreversible cathodic wave at $E_{pc,3} = -2.36$ V (vs SCE), where the reduction of the nitroso group takes place. It is possible to detect the formation of nitroso derivative after the third electron transfer, since appears new oxidation waves at $E_{pa} = -0.54$ V (vs SCE) and $E_{pa} = -0.21$ V in the anodic counter scan. These oxidation waves correspond to the oxidation of the nitroso and hidroxylamine derivatives radical anions to its neutral derivatives after the third reduction wave (Scheme 5). However, the current study will focus only on the first two electron transfers.

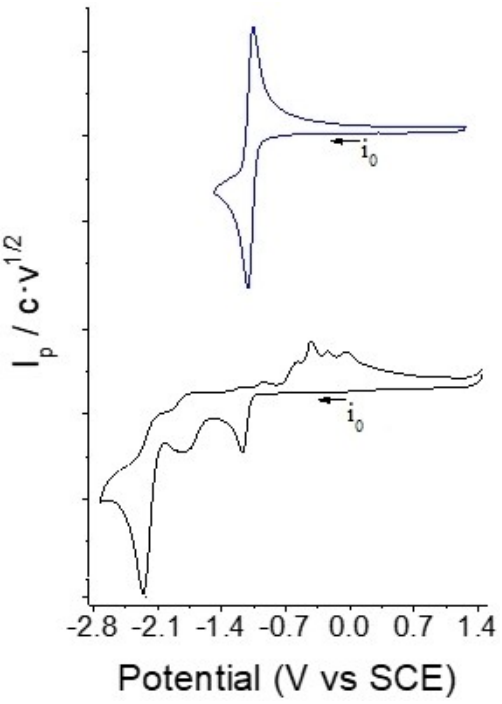

Figure 2. Cyclic voltammetry of 5.01 mM of **1** in DMF/0.1 M $TBABF_4$ at 15 °C, on a glassy carbon disk, under an inert atmosphere. Scan rate: 0.5 V·s^{-1}. Scan range: 0.0/−1.4/1.5/0.0 V (top), and Scan range: 0.0/−2.7/1.5/0.0 V third electron transfer (bottom).

2.1.1. Electrochemical Study of 1 Under an Inert Atmosphere at the First Electron Transfer

The first wave corresponds to the reversible reduction of **1**, so the compound takes a first electron reversibly, which is localized on the nitro group according to the value of the standard potential ($E^0 = -1.16$ V vs SCE) to form a radical anion, $\mathbf{1}^{\bullet-}$ (Figure 2). No oxidation products were detected after the reduction scan (Figure 2, blue scan).

© 2021 The Authors. ChemElectroChem published by Wiley-VCH GmbH

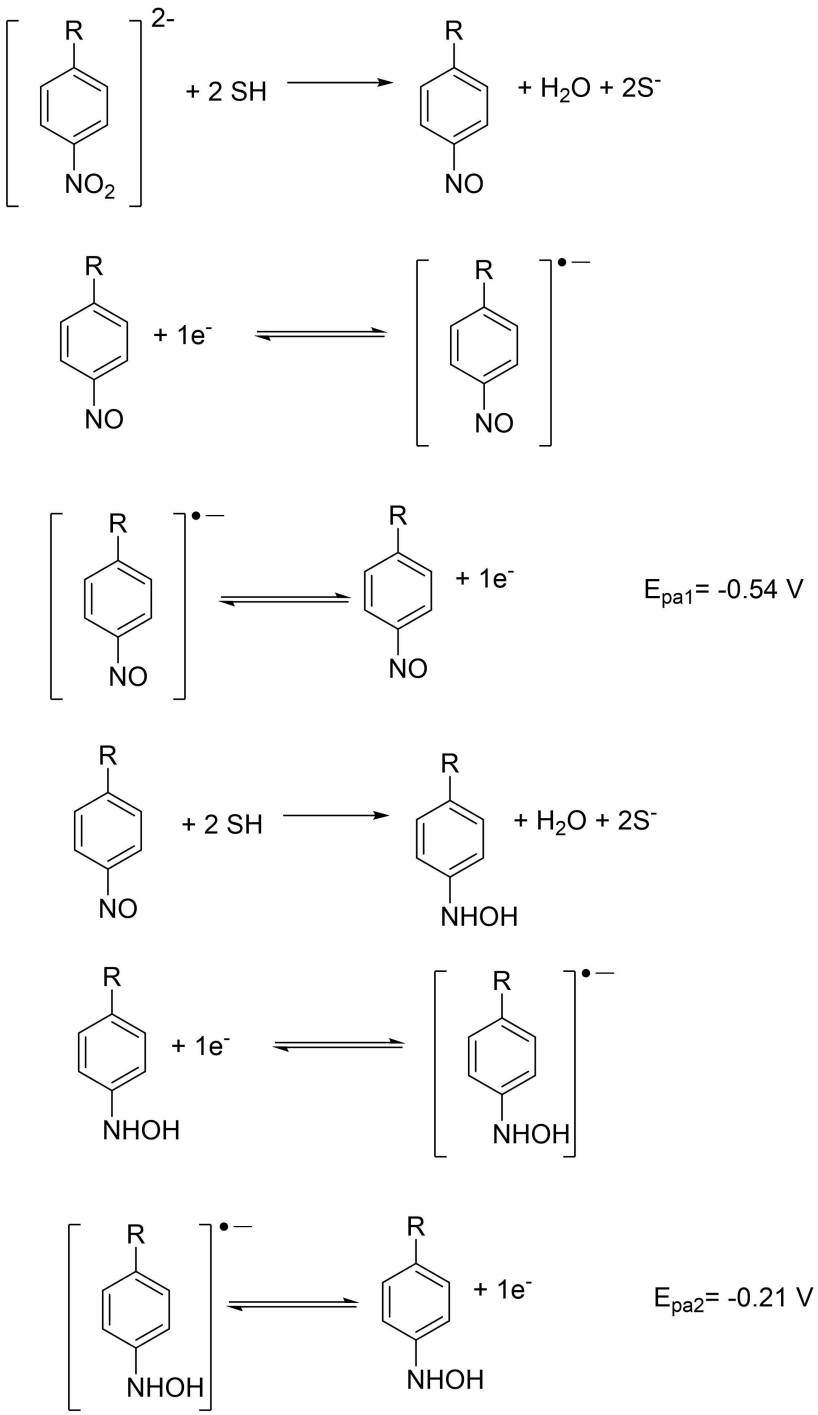

Scheme 5. Reduction mechanism of nitroaromatic derivates associated with the third reduction wave (where SH = solvent).

2.1.2. Electrochemical Study of 1 Under an Inert Atmosphere at the Second Electron Transfer

Figure 3, shows a second quasi-reversible monoelectronic wave at −2.00 V vs. SCE. The electrochemical behavior related to this second electron transfer is analyzed at different scan rates. Slow scan rates give an irreversible peak (Figure 3a), but when the scan rate was increased it became reversible (Figure 3b). Moreover, when the scan rate is slow, oxidation peaks are produced in an anodic scan after reduction at −0.33 V ($E_{pa,A}$) and −0.09 V ($E_{pa,B}$) vs. SCE, respectively.

In order to obtain the value of the electrochemical parameters of the second transfer of compound **1**, CVs at different scan rates were recorded in the same conditions. The reversibility of the second reduction wave is achieved at high scan rates (700 $V \cdot s^{-1}$), hence it is possible to determine the standard potential value of this second reduction process (E^0 =

© 2021 The Authors. ChemElectroChem published by Wiley-VCH GmbH

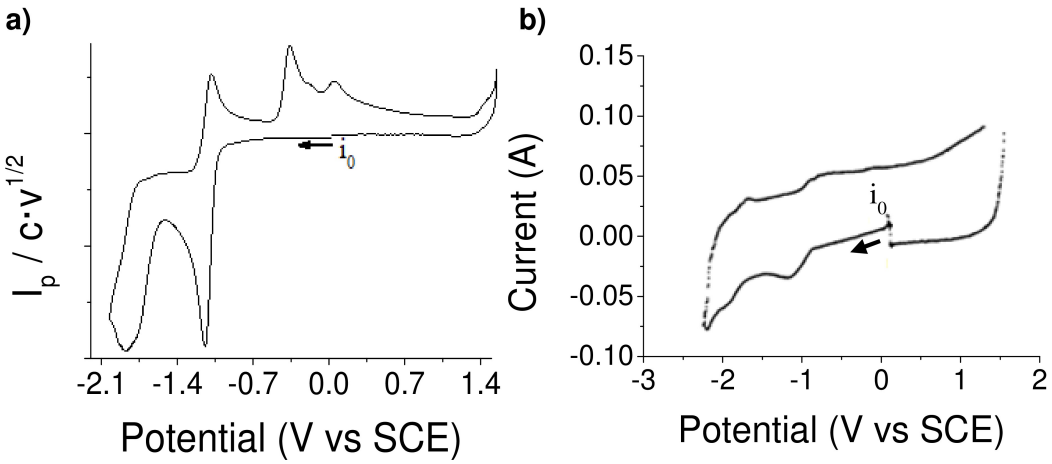

Figure 3. Cyclic voltammetry of 5.22 mM of **1** under an inert atmosphere at 15 °C. a) glassy carbon disk, Scan rate: 0.5 $V \cdot s^{-1}$, in DMF/0.1 M $TBABF_4$ b) glassy carbon disk ultra-micro-electrode ($\Phi = 9.7$ μm). Scan rate: 700 $V \cdot s^{-1}$, in DMF/0.6 M $TBABF_4$.

−1.63 V vs SCE). Note that the oxidation peaks related to the second electron transfer coupled reaction have disappeared (Figure 3b). Thus, we can propose that a chemical reaction is produced after the second electron transfer. The electrochemical parameters obtained for the second electron transfer were $E^0_2 = -2.63$ V, $k_s^{ap} = 9 \cdot 10^{-4}$ $cm \cdot s^{-1}$, $\alpha = 0.34$, and $k = 3 \cdot 10^4$ s^{-1} and were determined experimentally and confirmed by simulation of the experimental curves using the DIGISIM® software (Supporting information, Scheme S1 and Table S1).

A control potential electrolysis at $E_{ap} = -2.1$ V (vs SCE) was performed to determine the nature of the products obtained after the second electron transfer. After 2 F of charge and chemical treatment only, 16% of the reagent remained. The products obtained are summarized in Table 1.

Taking a close look at Table 1, the products obtained confirmed that the C–S cleavage is produced efficiently after passing the charge corresponding to two electrons. The main products obtained are 4-nitrotoluene and diphenyl disulfide, Ph–S–S–Ph. Moreover, aldehyde and dimer derivatives like 4,4′-dintrobibenzyl (D1) and 4,4′- dinitrostilbene (D2) were also detected.

Considering the products obtained after the electrolysis, it is possible to relate the oxidation peaks obtained at slow scan rates after the second electron transfer to the oxidation of nitrobenzyl anion[31] ($E_{pa,A} = -0.33$ V (vs SCE)), and thiophenolate anion oxidation[32] ($E_{pa,B} = -0.09$ V (vs SCE)). The second product was determined by comparison between it and CV obtained by commercial analogue, sodium thiophenolate, NaSPh (Figure 4, black line).

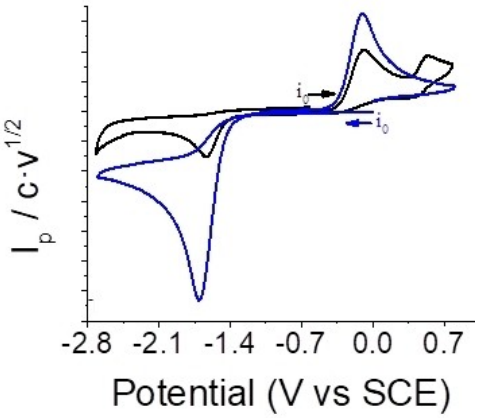

Figure 4. Cyclic voltammetry in DMF/0.1 M $TBABF_4$ at 15 °C, on a glassy carbon disk, under an inert atmosphere. Scan rate: 0.5 $V \cdot s^{-1}$. Solution of 5 mM of NaSPh (black line) and 5 mM of Ph–S–S–Ph (blue line).

Moreover, sodium thiophenolate electrochemical characterization showed two oxidation peaks ($E_{pa,1} = -0.09$ V vs SCE and $E_{pa,2} = +0.55$ V vs SCE) and a reduction wave at $E_{pc} = -1.64$ V (vs SCE). The first oxidation wave corresponds to the oxidation of sodium thiophenolate to its radical form, which could evolve following two different reaction pathways. It can either abstract a hydrogen atom leading to benzenethiol, which would be oxidized at $E_{pa} = +0.55$ V (vs SCE), or would evolve to dimerize into diphenyl disulfide, Ph–S–S–Ph, which has the reduction wave at $E_{pc} = -1.64$ V (vs SCE), Figure 5, blue line. This second pathway seems to be favored in the electrolysis of **1** because

Table 1. Results of electrochemical reduction of 1 under an inert atmosphere.

Entries	Electrolysis parameters		% Yield Product						
	E_{ap} [V]	Charge ($Q = nzF$)	**1**	Thiophenol	4-nitrotoluene	Ph–S–S–Ph	p-NO_2–Ph–CHO	D1	D2
1	−1.2	1F	100	–	–			–	–
2	−2.1	2F	16	11	34	36	3	18	4

© 2021 The Authors. ChemElectroChem published by Wiley-VCH GmbH

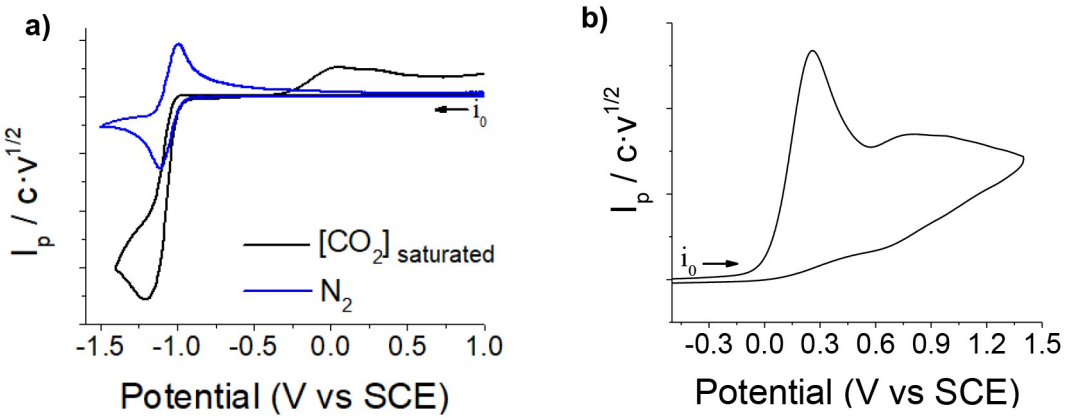

Figure 5. Cyclic voltammetry in DMF/0.1 M $TBABF_4$ at 15 °C on a glassy carbon disk. Scan rate: 0.5 $V \cdot s^{-1}$. Solution of 5 mM a) Compound **1** in saturated CO_2 atmosphere b) TBA_2Ox.

much more diphenyl disulfide (36% yield) is obtained than thiophenol (11% yield) with the passage of 2 F.

In the CV and electrolysis experiments, it is possible to propose a mechanism for the electrochemical reduction of **1**: an EEC mechanism (Scheme 6), in which compound **1** is reduced to obtain its radical anion, $\mathbf{1}\cdot^{-}$, with an electronic transfer (E), which is followed by another one (E), obtaining the dianion $\mathbf{1}^{2-}$, that is broken through a chemical reaction (C) in which there is C–S bond cleavage. This gives 4-nitrobenzyl and thiophenolate anions as products, which would eventually lead to nitrotoluene and thiophenol through a protonation reaction. Besides, PhS^- and nitrotoluene anion can reduce nitrotoluene by formation of a charge transfer complex during the electrolysis, which explains the formation of explains the presence of PhS–SPh, D1 and D2 as electrolysis products. A detailed description of the electrochemical reduction dimerization mechanism of nitrotoluene has been previously published by some of us.[33]

2.1.3. Thermodynamics and Kinetics of C–S Bond Cleavage

The experimental data (standard potentials E^0_1 and E^0_2, heterogeneous electron transfer rate constants, k_s, and first order constant, k) are treated following the theoretical model of dissociative electron transfer developed by Savéant.[34]

According to the thermodynamic cycle presented in Scheme 7, the standard free energy of the cleavage reaction is [Eq. (1)]:

$$\Delta_r G^0 = D_{NO_2PhCH_2SPh} + F\left(E^0_1 + E^0_2 - E^0_{(SPh^{\cdot})/(SPh)^-} - E^0_{NO_2PhCH_2^{\cdot}/NO_2PhCH_2^-}\right) - T\Delta_r S^0 \quad (1)$$

The D (bond dissociation energy) value is 218 $kJ\,mol^{-1}$, whereas the E^0 values are the previously determined of the subscript species, respectively. $\Delta_r S^0$ is approximately 1 $meV \cdot K^{-1}$ (96.5 $J \cdot K^{-1} \cdot mol^{-1}$). The effect of the solvent reorganization is considered negligible. The activation free energy $\Delta_r G^{\neq}$ is obtained from the first order constant, where the pre-exponential factor A is taken to be equal to $5 \cdot 10^{12}$ s^{-1} [Eq. (2)]:

$$k = A\exp\left(\frac{-\Delta_r G^{\neq}}{RT}\right) \quad (2)$$

The activation free energy, $\Delta_r G^{\neq}$, is related quadratically to the standard free energy of the cleavage reaction [Eq. (3)]:

$$\Delta_r G^{\neq} = \frac{4\Delta_r G^{0\neq}}{4}\left(1 + \frac{\Delta_r G^0}{4\Delta_r G^{0\neq}}\right)^2 \quad (3)$$

So, the standard activation free energy, $\Delta rG^{0\neq}$, is [Eq. (4)]:

$$\Delta_r G^{0\neq} = \frac{\Delta_r G^{\neq} - \frac{\Delta_r G^0}{2} + \sqrt{\left(\Delta_r G^{\neq} - \frac{\Delta_r G^0}{2}\right)^2 - \frac{(\Delta_r G^0)^2}{4}}}{2} \quad (4)$$

The results obtained using equation 1, confirms the exergonic character of the reaction cleavage at the dianion level ($\Delta_r G^{\circ} = -55.7$ $kJ \cdot mol^{-1}$) for compound **1**. Being the activation free energy, $\Delta_r G^{\neq}$, and standard activation free energy, $\Delta rG^{0\neq}$, 59.3 and 84.9 $kJ \cdot mol^{-1}$, respectively. Besides, as it is expected, a similar analysis at radical anion level reveals that the reaction cleavage is not thermodynamically favorable since the standard free energy ($\Delta_r G^{\circ} > 0$, Equation 5), which is in agreement with the above-mentioned electrochemical data [Eq. (5)].

$$\Delta_r G^0 = D_{NO_2PhCH_2SPh} + F\left(E^0_1 - E^0_{(SPh^{\cdot})/(SPh)^-}\right) - T\Delta_r S^0 \quad (5)$$

At this point, it is possible to envisage the electrochemical control of CO_2 reactivity by tuning the electrochemical reduction process of **1** in function of the applied potential. As the first electron transfer yields a stable radical anion, it is possible to use this reactant as a homogenous catalyst for CO_2 reduction. However, the second electron transfer yields carbon and sulfur anions, which can potentially react with CO_2 to yield carboxylate products (Scheme 8).

© 2021 The Authors. ChemElectroChem published by Wiley-VCH GmbH

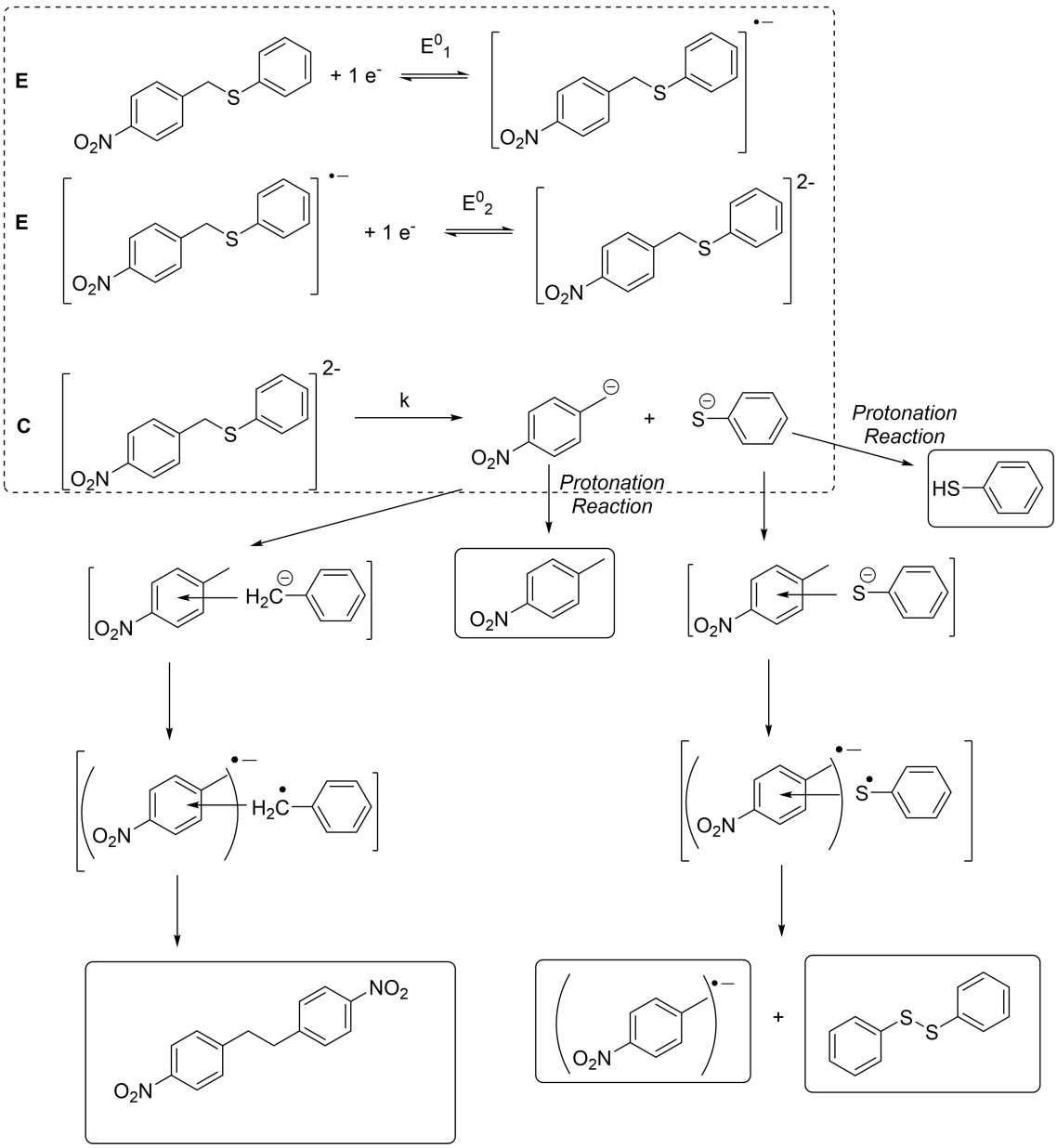

Scheme 6. Proposed EEC mechanism for the electrochemical reduction of **1**.

2.2. Electrochemical Study of 4-Nitrobenzyl Phenyl Thioether Under a CO_2 Saturated Atmosphere

The electrochemical behavior of 4-thionitrobenzyl phenyl thioether under a CO_2 atmosphere was completely different from its behavior under an inert atmosphere, and it could be divided into two reduction electron transfer processes.

2.2.1. The First Reduction Electron Transfer Process

Figure 5 shows the cyclic voltammetry response of **1** under a CO_2 saturated atmosphere. The first wave, which was reversible under an inert atmosphere, loses its reversibility, and its peak current values increase significantly when the solution is saturated with CO_2 (Figure 5a). These electrochemical features are characteristic of an electrocatalytic process in which compound **1** acts as a redox mediator (organic catalysts) in a homogeneous catalysis leading to a CO_2 reduction. It is important to note that, as far as we are aware, this is the lowest reduction potential value reported for reducing CO_2 using an organic compound as a mediator. The reduction potential value of CO_2 decreases to almost 1.0 V. On the other hand, the reduction potential of CO_2 in aprotic media is −2.2 V (vs SCE) in inert electrodes, which is very negative potential,[29] and also is reduced the potential in which CO_2 is directly reduced into its radical anion form, in almost 1 V.

© 2021 The Authors. ChemElectroChem published by Wiley-VCH GmbH

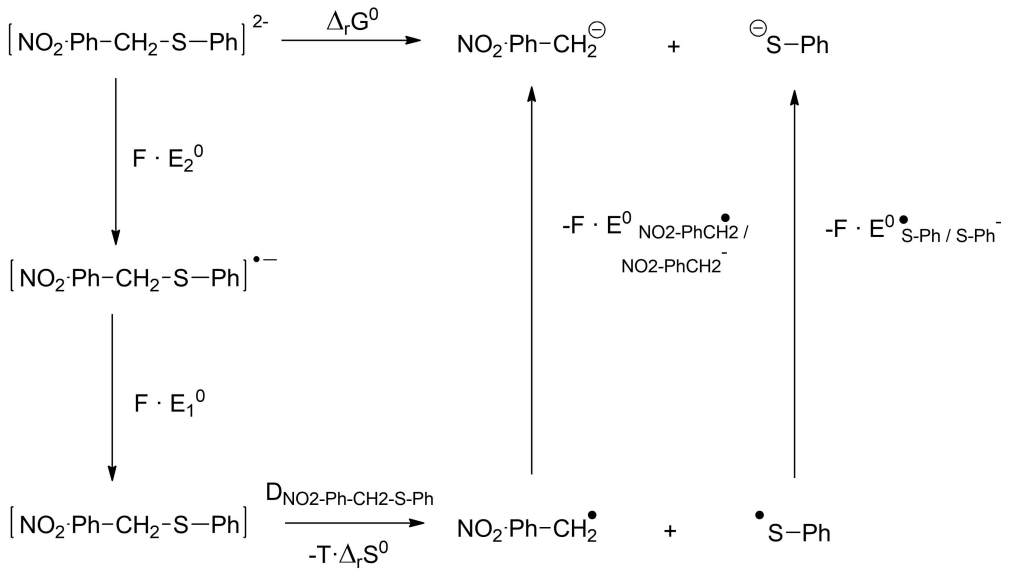

Scheme 7. Thermodynamic cycle for dianion cleavage.

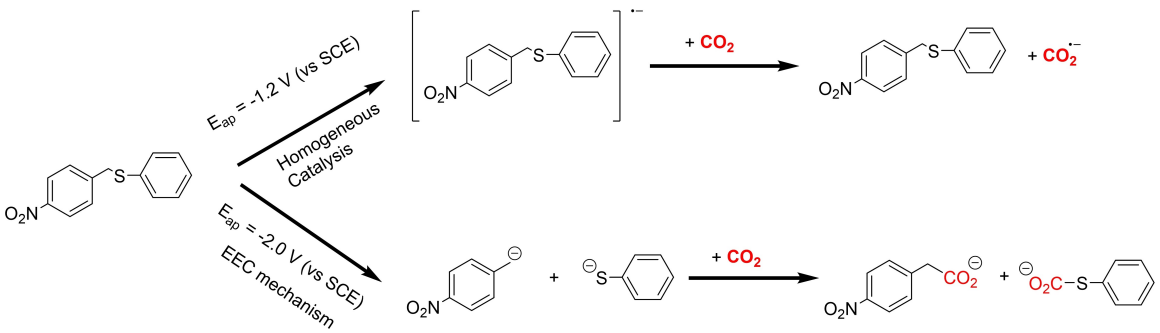

Scheme 8. Reactivity of **1** and CO_2 depending on the potential applied.

The new peak at $E_{pa} = +0.26$ V (vs SCE) is related to the oxidation of oxalate in aprotic media, which is in agreement with that of tetrabutylammonium oxalate, TBA_2Ox (Figure 5b), and in the literature.[35–37]

In order to determine the nature of the products obtained after the catalytic process, a control potential electrolysis was performed at $E_{ap} = -1.2$ V (vs SCE). The CO_2 reduction products were characterized in situ by Fourier transform infrared – attenuated total reflectance (FTIR-ATR) spectroscopy (Figure 6a)

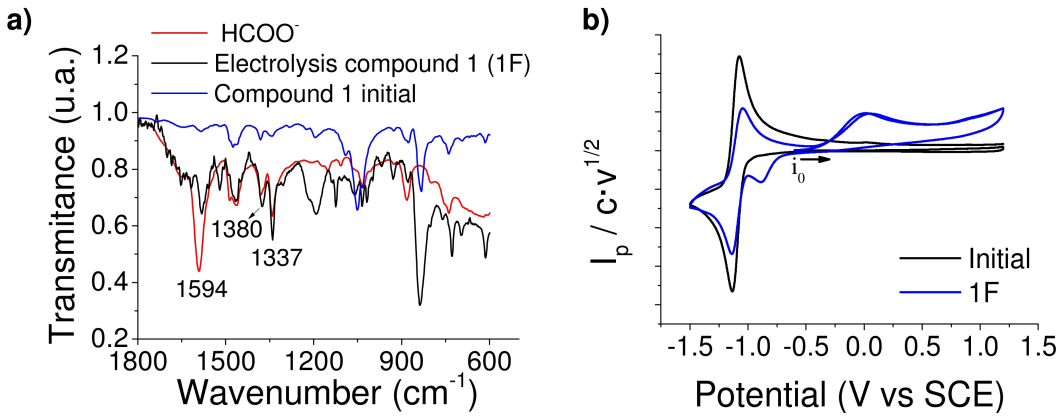

Figure 6. Characterization of compound 1 electrolysis a) IR (ATR) of formate pattern and electrolysis product of **1** b) Cyclic voltammogram of **1** (5.1 mM) in DMF/0.1 M $TBABF_4$ at 15 °C under an inert atmosphere. Glassy carbon disk. Scan rate: 0.5 V·s^{-1}.

© 2021 The Authors. ChemElectroChem published by Wiley-VCH GmbH

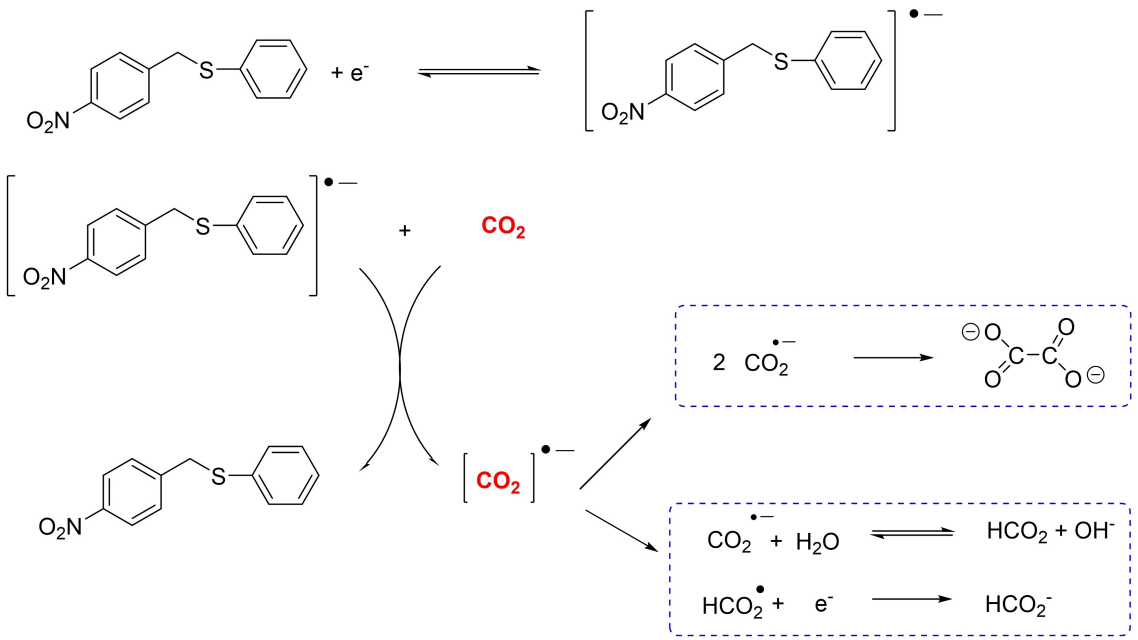

Scheme 9. Proposed mechanism for reducing compound **1** after the first electron transfer, under a CO_2 saturated atmosphere.

after the passage of 1 F. The IR data show new peaks at frequencies $\upsilon = 1594\ cm^{-1}$, $\upsilon = 1380\ cm^{-1}$, and $\upsilon = 1337\ cm^{-1}$, which would correspond with the formation of formate, $HCOO^-$.[38–40] The reduction process was monitored by cyclic voltammetry (Figure 6b). The cyclic voltammogram recorded at the end of the electrolysis showed two new peaks at anodic scan and cathodic scan related to the oxalate oxidation ($E_{pa} = +0.25$ V vs SCE), and a formate radical reduction formed on the oxalate oxidation ($E_{pc} = -0.89$ V vs SCE), respectively. It is important to note that 90% of compound **1** is recovered at the end of the process as a redox organic mediator. Therefore, compound **1** is reduced with an electron transfer giving a radical anion species that, through a homogeneous catalysis, would reduce CO_2 into a radical anion. This evolves into a formate anion and recovers the catalyst (Scheme 9). The production of formate after the control potential electrolysis seems to indicate that the presence of CO_2 in solution acidifies the reaction media.[41,42] Hence, two reduction electrochemical reduction mechanism are taking place at the same time. The generated CO_2 anion radical, after a one electron-transfer reduction at the electrode surface CO_2, can either dimerize leading to oxalate or be protonated yielding to formate (Scheme 9).

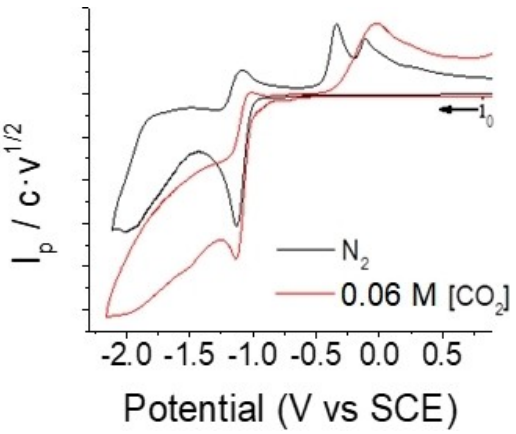

Figure 7. Cyclic voltammogram of **1** (5.1 mM) in DMF/0.1 M $TBABF_4$ at 15 °C, under inert atmosphere and 0.06 M CO_2 concentration. Glassy carbon disk. Scan rate: 0.5 $V \cdot s^{-1}$.

2.2.2. The Second Reduction Electron Transfer Process

After the second reduction wave of **1**, a completely different behavior is seen under a CO_2 atmosphere (Figure 7a). The cathodic scan shows that as the amount of CO_2 rises in the solution, the peak related to the first electron transfer loses its reversibility and increases its intensity, acting as an organic mediator in a catalysis process. At the same time, the peak related to the second electron transfer gets wider. However, the anodic peaks related to the C–S cleavage products change. The peak of nitrobenzyl anion oxidation, $E_{pa,A} = -0.33$ V (vs SCE), disappears as the CO_2 concentration increases in the solution. Moreover, the oxidation peak related to thiophenolate moves into more positive potentials and it may overlap with the oxalate oxidation peak.

Figure 8 shows a CV of sodium thiophenolate under a nitrogen and CO_2 atmosphere. It can be seen that the peak potential value related to its oxidation increases, as was previously described by Singh et al. for similar thiophenolate derivatives.[20] This can be explained by the formation of the corresponding carboxylate derivative ((phenylsulfanyl)formate, (Scheme 10)). Moreover, the oxidation of (phenylsulfanyl) formate makes it possible to deliver and recover the CO_2

© 2021 The Authors. ChemElectroChem published by Wiley-VCH GmbH

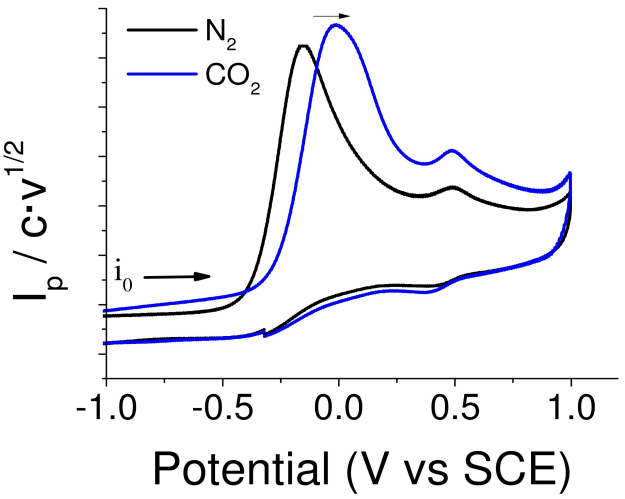

Figure 8. Cyclic voltammogram of thiophenolate, NaPhS, (5 mM) in DMF/0.1 M $TBABF_4$ at 15 °C. Glassy carbon disk. Scan rate: 0.5 $V \cdot s^{-1}$.

previously captured. Thus, the thiophenolate can act as a reversible CO_2 capture system that is electrochemically triggered.

A second electron transfer and a controlled potential electrolysis under a CO_2 atmosphere were performed to determine the nature of the products formed on the reduction obtained by **1**. Note that, at this point, it is expected to obtain products coming from the homogeneous catalysis, which is produced after the first electron transfer, as well as products arising from the electrocarboxylation through C–S cleavage, which occurs after the second electron transfer. Table 2 summarizes the products related to C–S cleavage reaction, the electrocarboxylate aromatic compound (**4**) was obtained in a 10% yield after the passage of 3F. Besides, in the electrolyzed solution formate was obtained in a 22 mM concentration. The yielding of this electrocatalytic CO_2 product involved a 5% of charge consumption. The nature of the products obtained was determined by nuclear magnetic resonance (^{1}H-NMR) and gas chromatography coupled with mass spectrometry (GC-MS).

At this point, it is possible to propose three different processes that occur at the same time. First, a homogeneous catalysis (radical anion level), which gives rise to a formate anion and the recovery of the reagent in a 40–50% yield, as explained in Scheme 9.

When a controlled potential electrolysis is performed at −2.3 V (vs SCE) (Table 2), C–S cleavage reaction takes place, leading to the corresponding carboxylated products, such as **3**, due to a nucleophile–electrophile reaction between CO_2 and the formed aromatic and sulfur anion moieties. Note that the nitro group is reduced to its amine analog, **3**.

According to the results in the literature, this may be due to an acidification of the electrolyte solvent due to CO_2 bubbling.[41,42] To analyze this effect, a controlled potential electrolysis of **1** was performed under the conditions depicted in Table 2, but adding one equivalent of acid ($HClO_4$) instead of CO_2, obtaining compound **4** with 10% yield after 2 F (Table 2, entry 1).

On the other hand, the dimer, diphenyl disulfide is obtained by radical-radical coupling of two units of thiophenyl radicals. These radicals are generated as a result of the oxidation of the (phenylsulfanyl)methanoate anion, which leads to the loss of CO_2 and the thiophenyl radical. This oxidation process could take place in the reaction with the oxygen in the air, probably during chemical treatment of the sample. Therefore, the (phenylsulfanyl)methanoate anion is not stable enough under these experimental conditions (Scheme 11).

3. Conclusions

The electrochemical reduction mechanism of 4-nitrobenzyl phenyl thioether, **1**, has been studied using electrochemical techniques, including cyclic voltammetry and control potential electrolysis under nitrogen and carbon dioxide atmospheres,

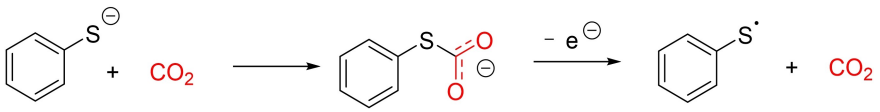

Scheme 10. Proposed mechanism for (phenylsulfanyl)formate oxidation.

Table 2. Results of electrochemical carboxylation of compound **1**.

Entries		Electrochemical parameters		Yield [%]			
		E_{ap} (V vs SCE)	Charge ($Q = znF$)	**1**	**2**	**4**	Carboxylation product **3**
1	N_2	−1.9[a]	2F	75	5	20	–
2	CO_2	−2.3	3F	48.7	41.3	–	10

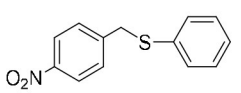

1

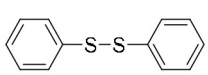

2

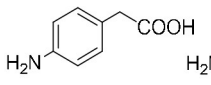

3

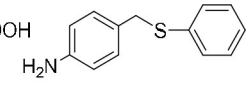

4

[a] Addion of 1 equivalent of $HClO_4$ to the acetonitrile solution

© 2021 The Authors. ChemElectroChem published by Wiley-VCH GmbH

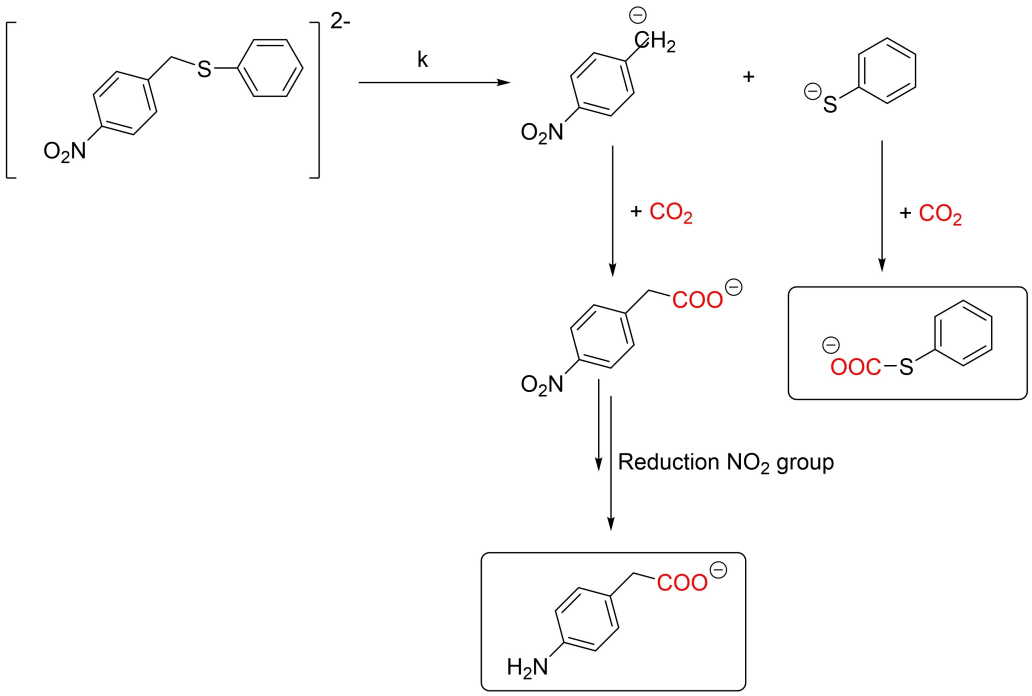

Scheme 11. Proposed mechanism for the electrochemical reduction of **1** under CO_2 at −2.3 V (vs SCE).

respectively. Its electrochemical reduction mechanism has been fully disclosed, and the thermodynamic and kinetics parameters determined. This study proves that the electrochemical reduction follows an EEC mechanism involving a C–S reaction cleavage that only takes place after the second electron transfer. Based on these data, compound **1** has been used for activating, valorizing and capturing CO_2. In this study CO_2 was reduced at −1.2 V through a catalytic process in which 4-nitrobenzyl phenyl thioether was an organic mediator. At the second reduction wave level (−2.3 V (vs SCE)), we took advantage of the C–S cleavage high-value added products, such as aminobenzylacetic acid, through the nucleophile–electrophile reaction between the nitrobenzyl anion and CO_2. Moreover, the electrogenerated thiophenolate anion can act as a reversible CO_2 capture and release system that is electrochemically triggered.

Acknowledgements

The authors thank the Ministerio de Ciencia e Innovación of Spain for financial support though the projects CTQ 2015-65439-R and PID2019-106171RB-I00. S.M. acknowledges the Autonomous University of Barcelona for her predoctoral PIF grant.

Conflict of Interest

The authors declare no conflict of interest.

Keywords: carbon–sulfur cleavage · electrochemistry · carbon dioxide · electrocarboxylation · homogeneous catalysis · CO_2 capture

[1] P. Roy, C. K. Manna, R. Naskar, T. K. Mondal, *Polyhedron* **2019**, *158*, 208–214.
[2] T. Liu, R. Qiu, L. Zhu, S. F. Yin, C. T. Au, N. Kambe, *Chem. Asian J.* **2018**, *13*, 3833–3837.
[3] K. Nogi, H. Yorimitsu, *Chem. Asian J.* **2020**, *15*, 441–449.
[4] P. J. Deuss, K. Barta, *Coord. Chem. Rev.* **2016**, *306*, 510–532.
[5] B. Du, W. Wang, Y. Wang, Z. Qi, J. Tian, J. Zhou, X. Wang, J. Han, J. Ma, Y. Pan, *Chem. Asian J.* **2018**, *13*, 404–408.
[6] G. Li, C. L. Ji, X. Hong, M. Szostak, *J. Am. Chem. Soc.* **2019**, *141*, 11161–11172.
[7] A. A. Isse, G. Berzi, L. Falciola, M. Rossi, P. R. Mussini, A. Gennaro, *J. Appl. Electrochem.* **2009**, *39*, 2217–2225.
[8] O. Lugaresi, A. Minguzzi, C. Locatelli, A. Vertova, S. Rondinini, C. Amatore, *Electrocatalysis* **2013**, *4*, 353–357.
[9] B. Huang, Y. Zhu, J. Li, G. Zeng, C. Lei, *Electrochim. Acta.* **2017**, *231*, 590–600.
[10] A. A. Isse, S. Gottardello, C. Durante, A. Gennaro, *Phys. Chem. Chem. Phys.* **2008**, *10*, 2409–2416.
[11] A. A. Isse, A. De Giusti, A. Gennaro, L. Falciola, P. R. Mussini, *Electrochim. Acta* 2006, 51, 4956–4964.
[12] P. W. Ayers, J. S. M. Anderson, J. I. Rodriguez, Z. Jawed, *Phys. Chem. Chem. Phys.* **2005**, *7*, 1918–1925.
[13] A. B. Meneses, S. Antonello, M. C. Arèvalo, F. Maran, *Electrochim. Acta* **2005**, *50*, 1207–1215.
[14] A. B. Meneses, S. Antonello, M. C. Arévalo, C. C. González, J. Sharma, A. N. Wallette, M. S. Workentin, *Chem. A Eur. J.* **2007**, *13*, 7983–7995.
[15] L. M. Bouchet, A. B. Peñéñory, M. Robert, J. E. Argüello, *RSC Adv.* **2015**, *5*, 11753–11760.
[16] S. A. Fleming, A. W. Jensen, *J. Org. Chem.* **1993**, *58*, 7135–7137.
[17] P. Maslak, J. Theroff, *J. Am. Chem. Soc.* **1996**, *118*, 7235–7236.
[18] J. Gu, J. Wang, J. Leszczynski, *J. Am. Chem. Soc.* **2006**, *128*, 9322–9323.
[19] S. A. Fleming, D. B. Rawlins, V. Samano, M. J. Robins, *J. Org. Chem.* **1992**, *57*, 5968–5976.
[20] P. Singh, J. H. Rheinhardt, J. Z. Olson, P. Tarakeshwar, V. Mujica, D. A. Buttry, *J. Am. Chem. Soc.* **2017**, *139*, 1033–1036.

© 2021 The Authors. ChemElectroChem published by Wiley-VCH GmbH

[21] O. Scialdone, A. Galia, G. Filardo, A. A. Isse, A. Gennaro, *Electrochim. Acta* **2008**, *54*, 634–642.
[22] A. Gennaro, C. M. Sánchez-Sánchez, A. A. Isse, V. Montiel, *Electrochem. Commun.* **2004**, *6*, 627–631.
[23] A. A. Isse, M. G. Ferlin, A. Gennaro, *J. Electroanal. Chem.* **2005**, *581*, 38–45.
[24] H. Senboku, A. Katayama, *Curr. Opin. Green Sustain. Chem.* **2017**, *3*, 50–54.
[25] R. Matthessen, J. Fransaer, K. Binnemans, D. E. De Vos, *J. Org. Chem.* **2014**, *10*, 2484–2500.
[26] I. Reche, S. Mena, I. Gallardo, G. Guirado, *Electrochim. Acta* **2019**, *320*, 134576.
[27] J. Luo, I. Larrosa, *ChemSusChem.* **2017**, *10*, 3317–3332.
[28] C. Amatore, J. M. Savéant, *J. Am. Chem. Soc.* **1981**, *103*, 5021–5023.
[29] A. Gennaro, A. A. Isse, J. M. Savéant, M. G. Severin, E. Vianello, *J. Am. Chem. Soc.* **1996**, *118*, 7190–7196.
[30] S. Mena, G. Guirado, *J. C.* **2020**, *6*, 34.
[31] M. Alvarez-Guerra, J. Albo, E. Alvarez-Guerra, A. Irabien, *Energy Environ. Sci.* **2015**, *8*, 2574–2599.
[32] M. Borsari, M. Cannio, G. Gavioli, *Electroanalysis* **2003**, *15*, 1192–1197.
[33] I. Gallardo, A. B. Gómez, G. Guirado, A. Lariño, M. Moreno, M. Ortigosa, S. Soler, *New J. Chem.* **2018**, *42*, 7005–7015.
[34] J. M. Savéant, *J. Phys. Chem.* **1994**, *98*, 3716–3724.
[35] M. M. Chang, T. Saji, A. J. Bard, *J. Am. Chem. Soc.* **1977**, *99*, 5399–5403.
[36] T. Kai, M. Zhou, S. Johnson, H. S. Ahn, A. J. Bard, *J. Am. Chem. Soc.* **2018**, *140*, 16178–16183.
[37] G. S. Rodman, A. J. Bard, *Inorg. Chem.* **1990**, *29*, 4699–4702.
[38] J. Gomes, S. Santos, J. Bordado, *Environ. Technol. (United Kingdom)* **2015**, *36*, 19–25.
[39] J. Desilvestro, S. Pons, *J. Electroanal. Chem.* **1989**, *267*, 207–220.
[40] E. R. Pérez, J. R. Garcia, D. R. Cardoso, B. R. McGarvey, E. A. Batista, U. P. Rodrigues-Filho, W. Vielstich, D. W. Franco, *J. Electroanal. Chem.* **2005**, *578*, 87–94.
[41] Y. A. Aubakirov, L. R. Sassykova, Z. K. Tashmukhambetova, S. Y. Karymbayev, S. Sendilvelan, M. Zharkyn, A. K. Zhussupova, A. A. Batyrbayeva, S. A. Kayrdynov, *Int. J. Biol. Chem.* **2018**, *11*, 89–98.
[42] J. Pearson, *Trans. Faraday Soc.* **1948**, *44*, 683.

Manuscript received: March 13, 2021
Revised manuscript received: April 14, 2021
Accepted manuscript online: April 28, 2021

© 2021 The Authors. ChemElectroChem published by Wiley-VCH GmbH